How to cite: *Angew. Chem. Int. Ed.* **2021**, *60*, 15482–15489
International Edition: doi.org/10.1002/anie.202103143
German Edition: doi.org/10.1002/ange.202103143

Sequence-Controlled Polymers **Hot Paper**

Degradation in Order: Simple and Versatile One-Pot Combination of Two Macromolecular Concepts to Encode Diverse and Spatially Regulated Degradability Functions

*Tiziana Fuoco**

Abstract: *The clever one-pot combination of two macromolecular concepts, ring-opening polymerization (ROP) and step-growth polymerization (SGP), is demonstrated to be a simple, yet powerful tool to design a library of sequence-controlled polymers with diverse and spatially regulated degradability functions. ROP and SGP occur sequentially at room temperature when the organocatalytic conditions are switched from basic to acidic, and each allows the encoding of specific degradable bonds. ROP controls the sequence length and position of the degradability functions, while SGP between the complementary vinyl ether and hydroxyl chain-ends enables the formation of acetal bonds and high-molar-mass copolymers. The result is the rational combination of cleavable bonds prone to either bulk or surface erosion within the same macromolecule. The strategy is versatile and offers higher chemical diversity and level of control over the primary structure than current aliphatic polyesters or polycarbonates, while being simple, effective, and atom-economical and having potential for scalability.*

Introduction

For a long time, aliphatic polyesters have had a leading position among the degradable polymers for biomedical applications.[1] Currently, their ability to degrade is valued outside the biomedical field as an opportunity to minimize the environmental pollution.[2] Indeed, degradability, the possibility for chemical recycling and utilization of renewable feedstock for the synthesis, make polyesters outstand also among sustainable polymers.[3]

Despite being considered degradable, the degradation process of for example, poly(lactide), PLA, and poly(ε-caprolactone), PCL, is a controversial matter. The complete degradation of PLA hardly occurs in the environment or in fresh and seawater.[4] While under hydrolytic and/or physiological conditions the physical properties are at the level of the demanded application for weeks to months, the erosion and complete biodegradation take from years to decades to occur. Therefore, a quite short service lifetime is followed by a long temporal gap during which, the polymer matrix remains in the service environment without being able to perform any function, lacking mechanical integrity. This process is described as heterogeneous bulk degradation and is typical of polyesters. The slower hydrolysis of the ester bonds than the rate of water uptake and their relative hydrophilicity result in hydrolytic chain scissions throughout the polymer bulk. The outcome is an exponential decrease of molar mass and an early loss of mechanical integrity which are however, accompanied by a negligible mass loss. The erosion rate further decreases when hardly degradable crystalline domains accumulate after the amorphous phase of the material has degraded.[5]

Several publications report the ring-opening copolymerization[6] of various monomers aiming to change the composition and the macromolecular structure of polyesters and speed up or slow down the bulk degradation process.[7] Although the synthesis of statistical copolyesters may seem sufficient to adjust the bulk properties of the resulting material for many applications, the elegant work of Meyer and colleagues demonstrated that, beyond composition, a precise design of the primary structure[8] has a tremendous impact on the macroscopic degradability outcome and could overcome the pitfalls of the heterogeneous bulk degradation.[9] Sequence-controlled poly(lactic acid-*co*-glycolic acid) showed indeed a linear degradation kinetics, different from the exponential decrease of the molar mass featured by the random counterpart. Nevertheless, the synthetic methodology was based on a tedious iterative process[10] impeding access to high molar mass and large-scale production and did not meet green chemistry principles, such as atom-economy and elimination of protection (and deprotection) strategies.

Despite the complexity of the factors governing degradation and erosion of polyesters,[1a] the degradation kinetics are determined by mechanisms that occur at molecular scale. The available options for material optimization are, for both of the above-described strategies, limited by the fact that degrada-

[*] Dr. T. Fuoco
Department of Fibre and Polymer Technology
School of Engineering Sciences in Chemistry, Biotechnology and Health, KTH Royal Institute of Technology
Teknikringen, 56–58, 100-44 Stockholm (Sweden)
E-mail: tiziana@kth.se

Supporting information (including comprehensive details of experimental procedures for the synthesis of polymers, characterization methods, tables of thermal analysis results, MALDI-ToF-MS calculations and mass loss, scheme of side reactions, NMR spectra, MALDI-ToF-MS spectra, and DSC thermograms) and the ORCID identification number(s) for the author(s) of this article can be found under:
https://doi.org/10.1002/anie.202103143.

tion arises exclusively from the hydrolytic cleavage of ester bonds.[5] Although the degradation time and profile are altered, none of the two approaches allows for changing or selecting the mechanism and the conditions in which degradation is triggered. Being able to trigger different degradation pathways by selective and orthogonal stimuli, would instead enhance the spatio-temporal regulation of the material properties depending on the surrounding environment.[11] Thus, to advance the applications' scope while enabling new abilities for degradable polymers, innovative synthetic routes should be identified to devise hybrid polyesters with controlled primary structure that begets programmable functions and performance, without sacrificing scalability and benignity.

Hence, the aim was to establish a simple, effective, versatile and atom-economical synthetic strategy to advance in sequence control of degradable polymers while precisely positioning diverse degradability functions. A very simple polymer chemistry was conceived to enable the design of a library of degradable polymers with higher, but properly devised, structural complexity and degradability functions' diversity than currently available aliphatic polyesters. The strategy rationally combines two traditional macromolecular concepts in one-pot, ring-opening polymerization (ROP) and step-growth polymerization (SGP), which occur neatly and sequentially by a simple catalyst switch. ROP and SGP each allow the encoding of specific and spatially regulated degradability functions able to undergo different degradation pathways, Figure 1.

The focus was on expanding the degradability functions from esters to reactive groups that enable surface erosion, such as acetal bonds.[12] Surface erosion ensures better control of long-term properties but it has not been hitherto achieved for polyesters.[5,13] The cleavage of acetal bonds is faster than water penetration in the polymer bulk and readily occurs under hydrolytic or acidic conditions forming lower molar mass, neutral compounds, prone to diffuse out of the polymeric surface and therefore, fostering surface erosion.[5] All these aspects differ from the bulk degradation of polyesters, and if both types of bonds are combined in the same chain, new degradability outcomes can be achieved, relevant to both biomedical[14] and widespread applications.[15] For instance, PLA chains including acetal bonds degraded in both distilled and seawater.[15a] These ester acetal copolymers were prepared by ROP of cyclic esters bearing an acetal moiety,[15a,16] which needed to be ad hoc synthesized and their copolymerization with other monomers does not allow the controlled positioning of the acetal groups along the chains.

Instead, the strategy developed here, combining ROP and SGP in a single synthetic procedure, allows the concomitant formation and controlled positioning of the acetal bonds during the polymerization, it is atom-economical, proceeds at rt and uses commercially available reagents and monomers. The approach is also more facile and straightforward than recently reported synthetic procedures to prepare polyesters with acid-sensitive ortho-ester groups along the chains.[17]

Results and Discussion

The general scheme of the synthetic strategy is reported in Figure 1 a. Ethylene glycol vinyl ether was identified as the simplest initiator that could meet the scope of the reaction

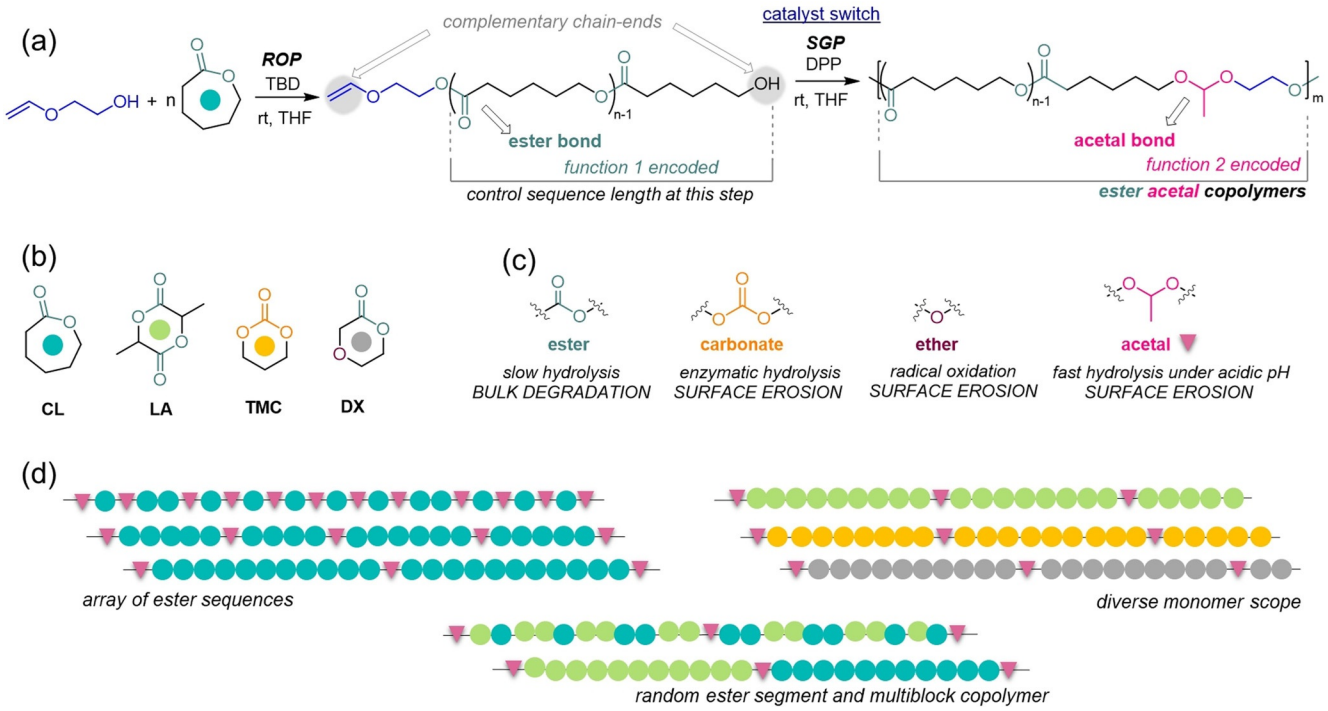

Figure 1. Scope and versatility of the developed approach. a) Reaction scheme of the polymerization approach combining two macromolecular concepts, i.e., ring-opening polymerization (ROP) followed by step-growth polymerization (SGP) with CL as model monomer; b) monomer scope; c) degradability functions incorporated along the macromolecules; and d) designed microstructures.

which was optimized using ε-caprolactone (CL) as monomer. 1,5,7-Triazabicyclo[4.4.0]dec-5-ene (TBD) was selected as the basic organocatalyst to promote the ROP of CL at rt[18] and in THF to yield vinyl ether oligoCL with controlled length and complementary chain-ends. Vinyl ethers are in fact stable under basic conditions and a basic catalyst was necessary to prevent side reactions of the initiator to form cyclic acetals (Scheme S1)[19] or premature SGP,[20] while allowing the synthesis of the envisioned vinyl ether oligoCL at rt. Changing the reaction conditions from basic to acidic by addition of an excess (3 equiv to TBD) of the Brønsted acid diphenyl phosphate (DPP) to the polymerization mixture, easily resulted in switching from ROP to SGP. The vinyl ether oligoCLs were therefore, the heterotelechelic macromonomers undergoing acid-catalyzed SGP between the complementary chain-ends. The mechanism is a Markovnikov direct addition of the -OH to the CH_2=CHO- producing acetal bonds.

Polyacetals can in fact be prepared by SGP of diols with di-vinyl ethers,[21,22] or of hydroalkyl vinyl ethers[20] in the presence of a strong acidic catalyst such as *p*-toluenesulfonic acid (PTSA) in relatively short times, 1–6 h, and with high molar mass. The weaker acidity of DPP ($pK_a \approx 3.7$–3.9)[23] than PTSA and the rt may justify the longer reaction time, 24–96 h, necessary to achieve high molar masses (Table 1). Although the ROP of CL also occurs in presence of DPP as catalyst,[18b] in the current polymerization system, the preferred polymerization pathway in acidic conditions is the reaction between the vinyl ether bond and the -OH chain ends, leading to SGP of the macromonomers and hence, the formation of the acetal bonds. In fact, by quenching the ROP step at ca. 85 mol% of CL conversion, it was observed by NMR analysis that the double bonds of the vinyl ether end groups were consumed and fully disappeared and the signals typical of the acetal groups appeared. On the contrary, the ratio of the CL monomer and CL units along the polymer chains remained almost constant during the course of the SGP, 2.5 mol% consumption of CL over 72 h (Figure S1).

The ratio of monomer to initiator, which was intentionally decided at the set-up polymerization step, regulated the length of the ester sequence produced by ROP and the position of the acetal bonds formed during SGP respectively, begetting sequence-control over the primary structure. If the primary structure of a copolymer is thoroughly controlled, it is possible to precisely dictate the bulk properties of the final material and its degradation profile. The versatility of the synthetic approach in designing different primary structures was proven by preparing an array of copolymers with increasing ester sequence length by varying the ratio of CL to ethylene glycol vinyl ether from 1:1 to 40:1 (Figure 1d; Table 1, entries 1–7). The ^{1}H NMR spectra of the vinyl ether oligoCL of different lengths and of the relative ester acetal copolymers are presented, along with the SEC data, in Figure 2. A thorough peak assignment[24] is provided in Figure S2.

The vinyl ether oligomers featured high end-group fidelity as indicated by the agreement between the integrals of the signals of the vinyl (=C*H*O-; 6.5 ppm) and the methylene (-CH_2OH; 3.6 ppm) protons. Their intensities decreased by increasing the amount of CL respect to the initiator (Figure 2a). MALDI-ToF MS analysis displayed a single population of species initiated from ethylene glycol vinyl ether, confirming the structure and end-group fidelity of the vinyl ether oligoCL (Figure S3).

The M_n values obtained by SEC analysis revealed a perfectly linear increase of the molar mass of the vinyl

Table 1: Ring-opening polymerization using ethylene glycol vinyl ether as initiator and sequential step-growth polymerization.[a]

Entry	Step I, ROP					Step II, SGP		
	Ratio CL:initiator	*t* [h]	Monomer conv. [%][b]	Oligomer length[c]	$M_{n,SEC}$ [g mol^{-1}] (*Đ*)[d,e]	*t* [h]	$M_{n,SEC}$ [g mol^{-1}] (*Đ*)[d,f]	No. acetal bonds[g]
1	1:1	0.5	>99	1.8	300 (1.6)	24	2300 (2.4)	8
2	1:1	4 min	>99	1.7	300 (1.4)	48	10900 (1.9)	36
3	5:1	4	>99	5.9	1600 (1.5)	96	44700 (1.7)	28
4	10:1	4	>99	10	3200 (1.4)	96	78400 (1.6)	25
5	20:1	4.5	91	18	5600 (1.4)	96	66700 (1.9)	11
6	30:1	4.5	80	23	7450 (1.2)	96	60500 (1.8)	8
7	40:1	4.5	86	33	10200 (1.4)	96	46000 (1.7)	4.5
8	10:1 (LA)[h,i]	2 h	99	8.2	1700 (1.9)	96	20550 (1.7)	7.3
9	10:1 (TMC)	2 h	99	9.2	2050 (1.9)	96	37500 (1.6)	18
10	10:1 (DX)[h,i]	2.5 h	85	8.3	1800 (2.1)	24	15550 (1.5)[j]	2.5
11	a 10:1 (LA)[h,i]	3.5 h	99	11	2200 (1.8)	48	11300 (1.8)	≈4.5
	b 10:1 (CL)][h]	3.5 h	99	11	2700 (1.5)			
12	5:5:1 (CL/LA)[i]	24 h	99	10.5	1400 (2.0)	48	15300 (1.7)	11

[a] Reaction conditions: CL = 20 mmol; THF = 5 mL; TBD = 0.11 mmol (0.5 mol% to monomer); ethylene glycol vinyl ether ranging from 20 mmol to 0.5 mmol; DPP = 0.32 mmol. [b] Conversion of monomer in vinyl ether oligomer determined from ^{1}H NMR spectra of the crude oligomerization mixtures. [c] Number of monomeric units constituting the vinyl ether oligomer, determined from ^{1}H NMR spectra of the crude oligomerization mixtures. [d] Number-average molar mass and dispersity determined by SEC ($CHCl_3$, 0.5 mL min^{-1}) vs. polystyrene standards. [e] SEC analysis performed on the crude polymerization mixture of the first step, ROP. No correction factors were utilized. [f] SEC analysis performed on the purified sample. [g] Number of acetal bonds as estimated by comparison of the M_n values of the ester acetal copolymer and the former vinyl ether oligoester. [h] Reaction performed in CH_2Cl_2. [i] TBD = 1 mol% to monomer. [j] The detected molar mass is probably an underestimation of the real molar mass of the sample: the value likely reflects only the low-molar-mass, soluble faction of the polymer, indeed, poly(*p*-dioxanone) has very poor solubility in $CHCl_3$ and, as the molar mass increases, the polymer precipitates.

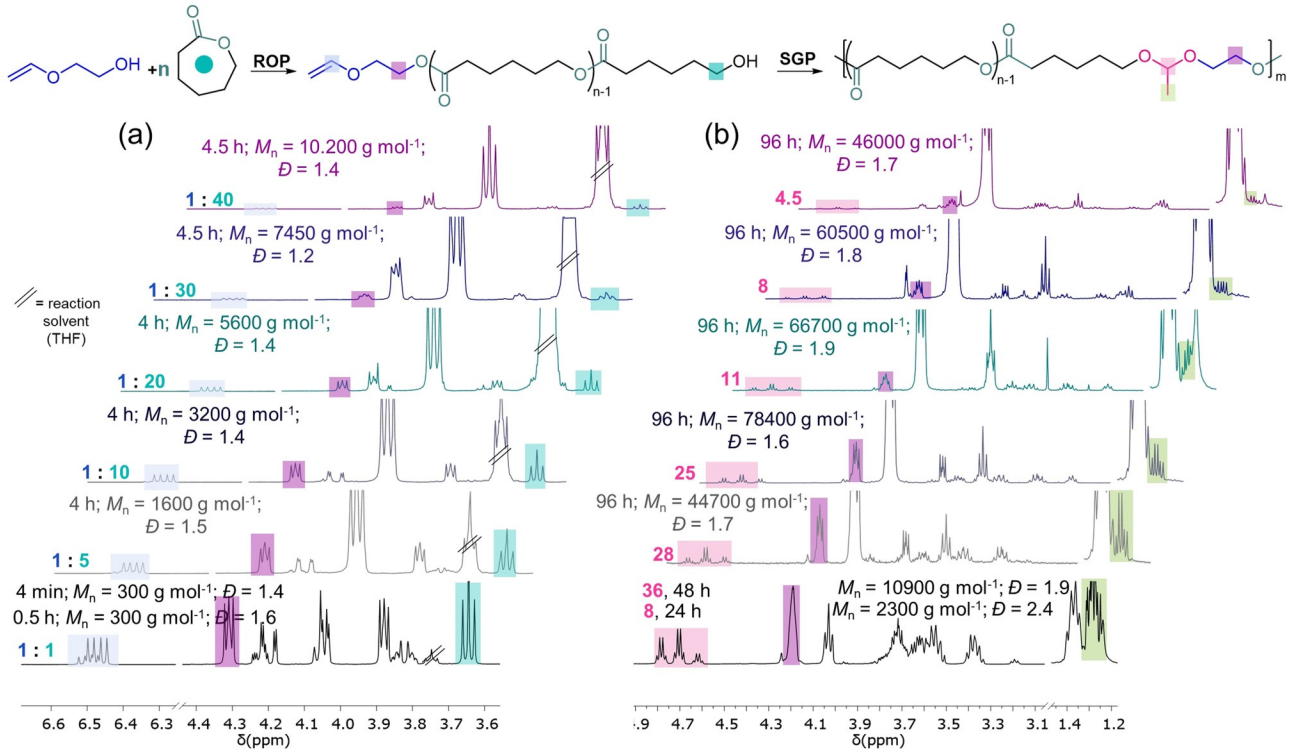

Figure 2. Array of ester acetal copolymers with increasing CL sequence length. ^{1}H NMR spectra (400 MHz, $CDCl_3$) of: a) the vinyl ether oligoCL prepared by ROP at different ethylene glycol vinyl ether to CL ratios as specified at the bottom left of each spectrum; b) the corresponding ester acetal copolymers obtained by SGP after catalyst switch, exhibiting a different number of acetal bonds as specified at the top left of each spectrum. Results obtained from SEC analysis (RI, $CHCl_3$ 0.5 mL min^{-1}, vs. polystyrene standards) are also reported for each sample after ROP and SGP (Table 1, entries 1–7).

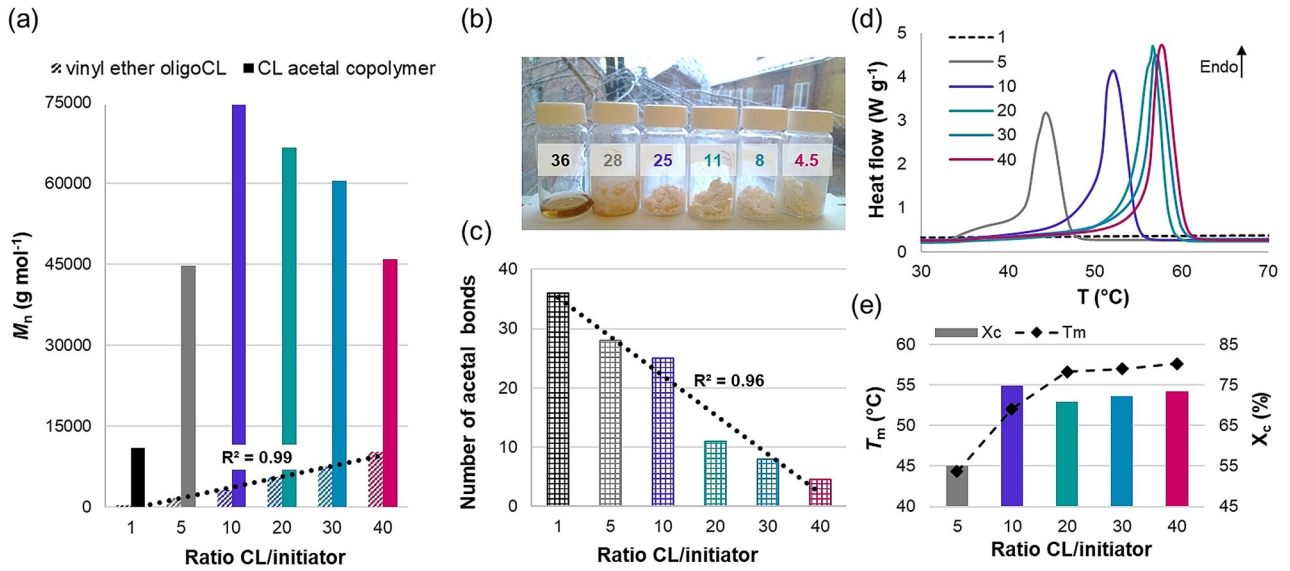

Figure 3. a) Number average molar mass (M_n) of the vinyl ether oligoCL and the corresponding ester acetal copolymers prepared at different CL to initiator ratios; b) photograph of the ester acetal copolymer samples with different numbers of acetal bonds and different ester sequence lengths; c) number of acetal bonds as a function of the catalyst to initiator ratio; d) DSC thermograms (I heating run) and e) melting point (T_m) and degree of crystallinity (X_c) of ester acetal copolymers prepared with different CL to initiator ratios.

ether oligoCL with increasing the ratio of monomer to initiator (Figure 3a). ^{1}H NMR analysis indicated that the 10:1 sample exhibited the best agreement between the oligoCL length and the ratio of the monomer to initiator. Lower ratio resulted, instead, in a higher number of units incorporated than the feed ratio, independently on the reaction time, indicating a faster rate of propagation than initiation in the presence of TBD.

Shorter lengths of the oligomer chain with respect to the theoretical value were calculated when the CL to initiator

ratio was higher than 10:1, due to the lower conversion of the monomer to oligomer (Table 1, entries 1–7). Although the dispersity ($Đ$) values in the range of 1.2–1.6 evidenced some deviation in the length of the vinyl ether oligomers (Figure 1, Table 1), these should be possible to be minimized in the future by exploring catalytic systems and/or reaction conditions that allow a living character of the ROP step and therefore, narrower dispersity.

The formation of the acetal groups by SGP was proven by the signals appearing between 4.9–4.6 ppm and 1.4–1.3 ppm and attributed[20] to the methine and methyl protons of the acetal moieties, respectively (Figure 2b), further confirmed by their ^1J correlation observed in the 2D COSY NMR spectrum (Figure S4).

Quantitative conversion of the macromonomers into ester acetal copolymers was indicated by the concomitant disappearance of the signals of the vinyl proton (=C*H*O-) at 6.5 ppm. The molar mass increased significantly after the SGP (Figure 3a), reaching the highest M_n value for the sample prepared with a 10:1 ratio. Longer polymerization time led to higher molar mass for the 1:1 sample (Table 1, entries 1 and 2). By keeping constant the reaction time of the SGP to 96 h, the molar mass values decreased by increasing the length of the vinyl ether oligoCL more than 10 CL units (Figure 3a), probably as a result of lower probability of acetal bonds formation due to the reduced number of chain-ends and slower diffusion of the longer oligomers (Table 1). Nevertheless, the positioning and number of the acetal bonds linearly decreased from 36 to 4.5 in agreement with the ratio of monomer to initiator (Figure 2b, Figure 3c), confirming the sequence regulation in encoding the degradable bonds. The highest number of acetal bonds per ester function and the prevalent formation of perfectly alternating ester acetal sequences for the copolymers prepared with 1:1 of CL to initiator ratio were confirmed by MALDI-ToF-MS analysis, Figure 4.

The sequence length and number of acetal bonds reflected on a change in the appearance and physical properties of the ester acetal copolymers (Figure 3b–e). The sample prepared at 1:1 ratio was amorphous, while samples prepared with higher CL:initiator ratio were semicrystalline and their melting point (T_m) augmented by lengthening the CL segments. The degree of crystallinity (X_c) increased from 5 to 10 CL units and was comparable for samples having longer CL segments (Figure 3d,e) being however, higher than the X_c of a high molar mass commercial PCL sample (Table S2). Differently from other polymers, the degree of crystallinity of PCL is lower for polymers of high molar mass.[25] Thus, the crystallinity of the ester acetal copolymers of CL might be affected by the molar mass, the CL sequence length and the presence of acetal groups, the last having a higher effect on T_m and therefore on increasing chain mobility. A higher chain mobility might explain the slightly higher X_c for the sample prepared at 10:1 ratio. Glass transition temperature (T_g) was instead not observed under the current experimental conditions (Table S2).

The positioning and number of acetal bonds, controlled by selecting the monomer to initiator ratio, reflect on the bulk properties of the materials and their erosion profile (Figure 5). The mass loss of films of selected ester acetal copolymers of CL was evaluated under hydrolytic conditions over 8 days and compared with a commercial PCL. Contrary to the PCL, each copolymer sample showed mass loss from the early stage of degradation and the erosion increased with the time and by tuning the quantity of acetal to ester functionalities. Indeed, given a certain time point, the mass loss values linearly decrease with the monomer to initiator ratio (Figure 5). The results indicate that surface erosion is favoured over bulk degradation and confirm that the sequence regulation achieved during the synthesis affords, under hydrolytic conditions, a controlled and predictable erosion rate. This behaviour is the opposite of the bulk

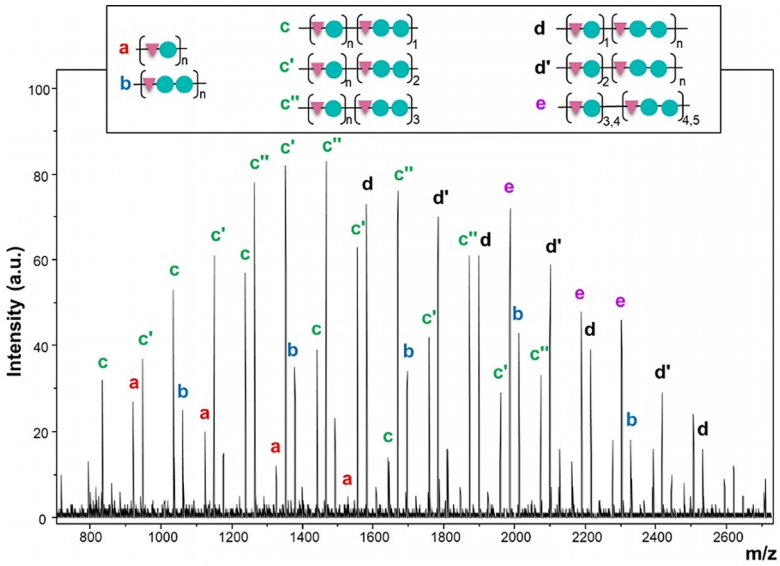

Figure 4. MALDI-ToF-MS analysis of the ester acetal copolymer prepared at a 1:1 monomer to initiator ratio (Table 1, entry 2). *m/z* values of the peak series are reported in Table S1.

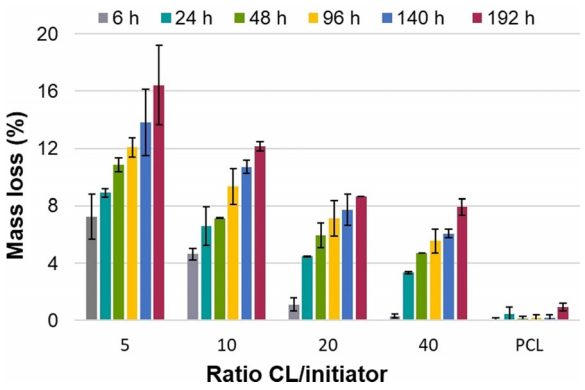

Figure 5. Mass loss (%) of selected ester acetal copolymers prepared at different CL to initiator ratios and compared to a commercial PCL. Values are listed in Table S3.

degradation of aliphatic polyesters, characterized by a long temporal gap between degradation and mass loss and by an unpredictable erosion profile.[1a,5,7]

To further expand the scope of the methodology and strengthen its potential in designing a library of different polymers, other monomers were evaluated (Figure 1 b,c) by keeping constant the ratio of monomer to initiator to 10:1, as it gave the best results for the polymerization of CL (Table 1, entries 8–10).

The polymerization procedure was extended to L-lactide (LA) evidencing the possibility of synthesizing copolymers having the same degradability functions as for the polymerization of CL, but with a different structure of the ester sequences. In this case, the formation of the acetal bonds entailed the attack of a secondary hydroxyl group on the vinyl bond, which due to steric reasons had probably lower reactivity than the primary -OH formed by ROP of CL. In fact, a lower molar mass was measured for the ester acetal copolymer prepared with LA compared with CL, although the total conversion of LA into the vinyl ether oligomers was achieved by ROP (Table 1, entries 4 and 8).

Proving the versatility of the strategy toward both structural and degradability function diversity, copolymers having carbonate segments and ether ester segments linked by spatially regulated acetal bonds were successfully synthesized by polymerizing trimethylene carbonate (TMC) and *p*-dioxanone (DX) respectively, Figure 1 b,c. Carbonate bonds are susceptible to enzymatic degradation, while ether bonds undergo radical oxidation, and both of them induce surface erosion.[5] Total conversion of TMC by ROP was achieved after 2 h and the carbonate acetal copolymer was successfully prepared with relatively high M_n, 37.5 kg mol^{-1}, and having on average 18 acetal bonds per chain at a distance of 9 TMC units. Slightly lower conversion, 85 %, was reached after 2.5 h for the ROP of DX, and a lower molar mass was measured for the relative ester ether acetal copolymers (Table 1, entries 9 and 10), most likely due to poor solubility of the polymer at increased molar mass. In other words, the low M_n value obtained by SEC probably accounts only for the low molar mass soluble faction in $CHCl_3$. Indeed, precipitation of the polymer was observed during the SGP and therefore, the reaction was terminated after 24 h. Besides the increase in molar mass observed by SEC after the SGP step, the formation of the envisaged copolymers was supported by NMR analysis for all the four monomers. For instance, along with the signals of the repeating CL, LA, TMC or DX monomeric units, the peaks attributed to the methine and methyl carbons of the acetal groups were detected in the range of 100–99 and 20–19 ppm of the ^{13}C NMR spectra, respectively (Figure S5).

Thermal analysis showed that only the copolymer prepared by polymerization of DX was semicrystalline. While, the T_g values of the three copolymers prepared by polymerization of LA, TMC and DX, were, respectively 20.6, −34.3 and −17.4 °C, lower than the T_g values usually observed for the corresponding homopolymers (Table S2, entries 8–10).[26] An analogous influence of the acetal groups on the T_g has also been recently observed for random copolymers of lactide and 1,3-dioxolane.[27]

More complex primary structures were also achieved implementing the same strategy (Figure 1 d, Figure 6).

Vinyl ether oligo CL and vinyl ether oligoLA were prepared in two separate reaction vessels with identical length (10:1 monomer to initiator ratio) and therefore, similar M_n. After complete conversion of the monomers, the two reaction solutions were combined and the reaction conditions switched to SGP to yield a multiblock copolymer, where each block consisted of either CL or LA segment spaced by the acetal moieties (Figure 6 a; Table 1, entry 11). The increase in the absolute value of M_n and the monomodal molar mass distribution observed after the SGP step suggested the formation of the envisaged copolymer architecture, further confirmed by DOSY NMR where the signals of the LA and CL segments lied at the same diffusion coefficient thus, they belonged to the same polymeric chain (Figure 6 c). In contrast, a vinyl ether oligo(CL-*ran*-LA) with an average of 10.5 monomeric units was obtained from the random oligomerization of a 50:50 mixture of CL and LA in presence of ethylene glycol vinyl ether, which underwent SGP forming a random CL/LA copolymer with acetal bonds discretely positioned every 10.5 ester units (Figure 6 b; Table 1, entry 12). The primary structure of the synthesized copolymers, was confirmed by analysis of the methine and methylene regions of their ^{13}C NMR spectra. Signals attributable to consecutive LA-LA and CL-CL homosequences were solely observed for the multiblock copolymers, while signals attributable to LA-CL and CL-LA heterosequences were detected for the copolymer consisting of random CL/LA segments confirming the statistical arrangement of the ester monomeric units (Figure 6 d).

The difference in the primary structures reflected on the thermal properties of the copolymers (Figure S6). The multiblock copolymer was semicrystalline with a T_m similar to the ester acetal copolymer prepared by polymerization of CL, indicating the ability of the long CL segments to crystallize. The random copolymer was instead amorphous with a T_g much lower than the analogous copolymer prepared by polymerizing LA only, a consequence of the statistical arrangement of the two monomeric units (Figure S5).

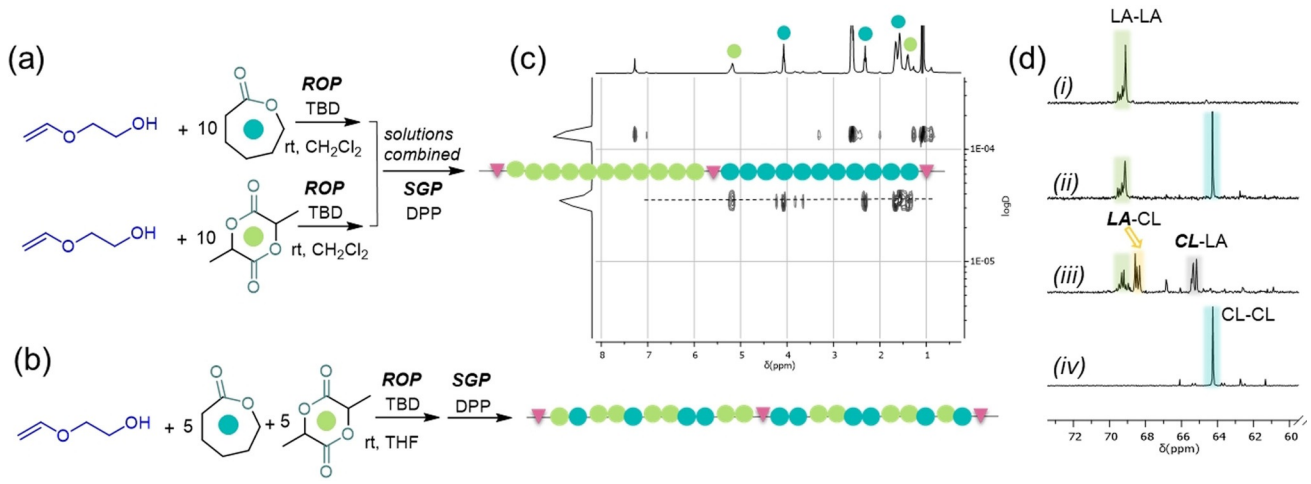

Figure 6. Reaction scheme for the synthesis of a) multiblock and b) random ester acetal copolymers of CL and LA. c) DOSY NMR spectra (400 MHz, $CDCl_3$) of the multiblock LA/CL copolymer with spatially regulated acetal bonds. d) Selected region of ^{13}C NMR spectra (101 MHz, $CDCl_3$) of (i) ester acetal copolymer of LA; (ii) multiblock ester acetal copolymer of LA and CL; (iii) random ester acetal copolymer of LA and CL; and (iv) ester acetal copolymer of CL (Table 1, entries 4, 8, 11, and 12).

The results evidence the broad application scope of the strategy and signify that the physio-chemical properties of the final polymer, such as morphology, degree of crystallinity, surface hydrophobicity or hydrophilicity, degradation rate and mechanism, are all aspects that could be in principle decided at the set-up polymerization step by selecting the monomer (or combination of them), the ratio of monomer(s) to initiator and/or by designing different microstructures. These findings open up for new opportunities to control structure and macroscopic properties, advancing the field of both sequence-controlled and degradable polymers.

Conclusion

The clever one-pot combination of sequential ROP and SGP enabled sequence-controlled copolymers to be neatly created and diverse degradability functions to be manipulated in a rational way. A higher level of control of the primary structure and higher chemical diversity than classical ring-opening copolymerization approaches were achieved in a single synthetic procedure, which reflected on the properties of the copolymers and their degradation profile. The developed strategy offers advantages such as (i) high versatility of the structures and control on the positioning of the degradability functions; (ii) high molar mass polymers; (iii) ease of synthesis; (iv) atom-economy; (v) the possibility of performing the reaction at room temperature. Moreover, it does not require protection (and deprotection) strategies, and uses organocatalysts and inexpensive, commercially available reagents and monomers. These remarkable aspects meet green chemistry principles and should enable the combination of chemical diversity and controlled design of degradable macromolecules with scalability. Further implementations are ongoing to unlock the design of hybrid polyesters able to degrade through different and controlled mechanisms such as surface erosion.

Acknowledgements

The Swedish Research Council (VR Starting Grant n. 2020-03247) is acknowledged for financial support.

Conflict of interest

The authors declare no conflict of interest.

Keywords: atom economy · degradation · ring-opening polymerization · sequence-controlled polymers · step-growth polymerization

[1] a) L. N. Woodard, M. A. Grunlan, *ACS Macro Lett.* **2018**, *7*, 976–982; b) D. Pappalardo, T. Mathisen, A. Finne-Wistrand, *Biomacromolecules* **2019**, *20*, 1465–1477.
[2] T. P. Haider, C. Völker, J. Kramm, K. Landfester, F. R. Wurm, *Angew. Chem. Int. Ed.* **2019**, *58*, 50–62; *Angew. Chem.* **2019**, *131*, 50–63.
[3] D. K. Schneiderman, M. A. Hillmyer, *Macromolecules* **2017**, *50*, 3733–3749.
[4] G.-X. Wang, D. Huang, J.-H. Ji, C. Völker, F. R. Wurm, *Adv. Sci.* **2021**, *8*, 2001121.
[5] B. Laycock, M. Nikolić, J. M. Colwell, E. Gauthier, P. Halley, S. Bottle, G. George, *Prog. Polym. Sci.* **2017**, *71*, 144–189.
[6] A.-C. Albertsson, I. K. Varma, *Biomacromolecules* **2003**, *4*, 1466–1486.
[7] a) T. Fuoco, A. Finne-Wistrand, *Biomacromolecules* **2019**, *20*, 3171–3180; b) T. Fuoco, T. Mathisen, A. Finne-Wistrand, *Polym. Degrad. Stab.* **2019**, *163*, 43–51.
[8] C. M. Thomas, J.-F. Lutz, *Angew. Chem. Int. Ed.* **2011**, *50*, 9244–9246; *Angew. Chem.* **2011**, *123*, 9412–9414.
[9] a) J. Li, R. M. Stayshich, T. Y. Meyer, *J. Am. Chem. Soc.* **2011**, *133*, 6910–6913; b) J. Li, S. N. Rothstein, S. R. Little, H. M. Edenborn, T. Y. Meyer, *J. Am. Chem. Soc.* **2012**, *134*, 16352–16359.
[10] R. M. Stayshich, T. Y. Meyer, *J. Am. Chem. Soc.* **2010**, *132*, 10920–10934.

[11] a) K. A. Miller, E. G. Morado, S. R. Samanta, B. A. Walker, A. Z. Nelson, S. Sen, D. T. Tran, D. J. Whitaker, R. H. Ewoldt, P. V. Braun, S. C. Zimmerman, *J. Am. Chem. Soc.* **2019**, *141*, 2838 – 2842; b) T.-G. Hsu, J. Zhou, H.-W. Su, B. R. Schrage, C. J. Ziegler, J. Wang, *J. Am. Chem. Soc.* **2020**, *142*, 2100 – 2104; c) Y. Lin, T. B. Kouznetsova, S. L. Craig, *J. Am. Chem. Soc.* **2020**, *142*, 2105 – 2109; d) A.-C. Albertsson, M. Hakkarainen, *Science* **2017**, *358*, 872 – 873; e) Q. Zhang, Z. Hou, B. Louage, D. Zhou, N. Vanparijs, B. G. De Geest, R. Hoogenboom, *Angew. Chem. Int. Ed.* **2015**, *54*, 10879 – 10883; *Angew. Chem.* **2015**, *127*, 11029 – 11033.

[12] G. Herwig, A. P. Dove, *ACS Macro Lett.* **2019**, *8*, 1268 – 1274.

[13] A. Göpferich, *Biomaterials* **1996**, *17*, 103 – 114.

[14] L. Bixenmann, J. Stickdorn, L. Nuhn, *Polym. Chem.* **2020**, *11*, 2441 – 2456.

[15] a) R. T. Martin, L. P. Camargo, S. A. Miller, *Green Chem.* **2014**, *16*, 1768 – 1773; b) S. A. Miller, *ACS Macro Lett.* **2013**, *2*, 550 – 554.

[16] a) A. E. Neitzel, T. J. Haversang, M. A. Hillmyer, *Ind. Eng. Chem. Res.* **2016**, *55*, 11747 – 11755; b) A. E. Neitzel, L. Barreda, J. T. Trotta, G. W. Fahnhorst, T. J. Haversang, T. R. Hoye, B. P. Fors, M. A. Hillmyer, *Polym. Chem.* **2019**, *10*, 4573 – 4583; c) A. E. Neitzel, M. A. Petersen, E. Kokkoli, M. A. Hillmyer, *ACS Macro Lett.* **2014**, *3*, 1156 – 1160.

[17] a) Y. Xing, Z. Xu, T. Liu, L. Shi, D. Kohane, S. Guo, *Angew. Chem. Int. Ed.* **2020**, *59*, 7235 – 7239; *Angew. Chem.* **2020**, *132*, 7302 – 7306; b) M. J.-L. Tschan, N. S. Ieong, R. Todd, J. Everson, A. P. Dove, *Angew. Chem. Int. Ed.* **2017**, *56*, 16664 – 16668; *Angew. Chem.* **2017**, *129*, 16891 – 16895.

[18] a) R. C. Pratt, B. G. G. Lohmeijer, D. A. Long, R. M. Waymouth, J. L. Hedrick, *J. Am. Chem. Soc.* **2006**, *128*, 4556 – 4557; b) T. Fuoco, T. T. Nguyen, T. Kivijärvi, A. Finne-Wistrand, *Eur. Polym. J.* **2020**, *141*, 110098.

[19] E. Cabianca, F. Chéry, P. Rollin, A. Tatibouët, O. De Lucchi, *Tetrahedron Lett.* **2002**, *43*, 585 – 587.

[20] H. Zhang, E. Ruckenstein, *J. Polym. Sci. Part A* **2000**, *38*, 3751 – 3760.

[21] J. Heller, D. W. H. Penhale, R. F. Helwing, *J. Polym. Sci. Polym. Lett. Ed.* **1980**, *18*, 293 – 297.

[22] a) A. Moreno, G. Lligadas, J. C. Ronda, M. Galià, V. Cádiz, *Polym. Chem.* **2019**, *10*, 5215 – 5227; b) R. Tomlinson, M. Klee, S. Garrett, J. Heller, R. Duncan, S. Brocchini, *Macromolecules* **2002**, *35*, 473 – 480.

[23] P. Christ, A. G. Lindsay, S. S. Vormittag, J.-M. Neudörfl, A. Berkessel, A. C. O'Donoghue, *Chem. Eur. J.* **2011**, *17*, 8524 – 8528.

[24] a) C. Iojoiu, D. Cade, H. Fessi, T. Hamaide, *Polym. Int.* **2006**, *55*, 222 – 228; b) K. V. Zaitsev, Y. A. Piskun, Y. F. Oprunenko, S. S. Karlov, G. S. Zaitseva, I. V. Vasilenko, A. V. Churakov, S. V. Kostjuk, *J. Polym. Sci. Part A* **2014**, *52*, 1237 – 1250.

[25] M. J. Jenkins, K. L. Harrison, *Polym. Adv. Technol.* **2006**, *17*, 474 – 478.

[26] a) A. Meduri, T. Fuoco, M. Lamberti, C. Pellecchia, D. Pappalardo, *Macromolecules* **2014**, *47*, 534 – 543; b) Z. Zhang, R. Kuijer, S. K. Bulstra, D. W. Grijpma, J. Feijen, *Biomaterials* **2006**, *27*, 1741 – 1748; c) K.-K. Yang, X.-L. Wang, Y.-Z. Wang, *J. Macromol. Sci. Polym. Rev.* **2002**, *42*, 373 – 398.

[27] B. Kost, M. Basko, *Polym. Chem.* **2021**, *12*, 2551 – 2562.

Manuscript received: March 3, 2021
Accepted manuscript online: May 5, 2021
Version of record online: June 9, 2021

